

UC Berkeley

Research Reports

Title

An Experimental Study On Lateral Control Of A Vehicle

Permalink

<https://escholarship.org/uc/item/3rr9371v>

Authors

Hessburg, Thomas

Peng, Huei

Tomizuka, Masayoshi

et al.

Publication Date

1991

CALIFORNIA PATH PROGRAM
INSTITUTE OF TRANSPORTATION STUDIES
UNIVERSITY OF CALIFORNIA AT BERKELEY

An Experimental Study on Lateral Control of a Vehicle

**Thomas Hessburg
Huei Peng
Masayoshi Tomizuka
Wei-Bin Zhang**

**PATH Research Report
UCB-ITS-PRR-91-17**

This work was performed as part of the California PATH Program of the University of California, in cooperation with the State of California, Business and Transportation Agency, Department of Transportation, and the United States Department of Transportation, Federal Highway Administration.

The contents of this report reflect the views of the authors who are responsible for the facts and the accuracy of the data presented herein. The contents do not necessarily reflect the official views or policies of the State of California. This report does not constitute a standard, specification, or regulation.

August 199 1

ISSN 1055-1425

This paper has been mechanically scanned. Some errors may have been inadvertently introduced.

An Experimental Study on Lateral Control of a Vehicle

Thomas Hessburg, Hwei Peng, Masayoshi Tomizuka, and Wei-Bin Zhang

August 30, 1991

Abstract

The work presented in this paper addresses issues regarding the implementation of an integration of several specific technologies involved in achieving lateral guidance of an experimental automotive vehicle on an automated highway. Results demonstrate the feasibility of the proposed discrete magnetic marker reference/sensing system. In addition, the performance and limitations of a PID/feedforward controller is investigated with respect to tracking accuracy of straight and curved sections as well as robustness to changes in load, longitudinal velocity, and cornering stiffness.

1 Introduction

A number of technologies must be integrated in order to realize lateral guidance of a vehicle on an automated highway. The first such technology is a roadway reference/sensing system. Its purpose is to accurately and reliably provide the lateral controller with information about the lateral displacement of the vehicle from the center of the roadway, as well as geometrical characteristics of the roadway. "Roadway geometry" information may include current as well as a finite amount of future information. Among several possible methods for a roadway reference system, a discrete magnetic marker scheme is proposed as the system in the present study [1]. The advantages of this method include the ease of transmission and storage of discrete elements of information, the use of possible binary codes within the markers to describe future information on roadway geometry, and the flexibility and economic attractiveness of roadway installation and maintenance, as compared to alternative referencing methods.

Another technology is the formulation of the control law. The objectives of the controller are to achieve good vehicle tracking to the center of the lane while maintaining smooth ride quality in terms of lateral motion. These objectives should be met over a reasonable range of operating conditions pertaining to vehicle speed, load, and cornering stiffness, which is a parameterization of traction between the tire and road surface. It is assumed that the controller has access to current and future roadway curvature information (for a finite length of roadway) in terms of the radius of curvature and the direction.

The Program on Advanced Technology for the Highway (PATH) has, among several other research topics, developed research in the above two technologies [1,2]. The purpose of this work is to integrate and apply the discrete magnetic marker reference/sensing system and a proposed control law to an actual experimental automotive system. The accuracy of the reference/sensing system as well as the performance of the control law is evaluated over a range of extreme operating conditions. It will be shown that a simple fixed gain PID control law is not sophisticated enough to achieve acceptable tracking on curved sections of roadway. Furthermore, although the addition of a feedforward compensator improves the tracking performance, the modified controller is still unable to meet **all** the stated control objectives.

A summary of the reference/sensing system, the dynamic model, the control law, and the experimental car will be presented in the following sections. The final sections include the experimental procedure, results, and discussion.

2 Lateral Displacement Measurement

The magnetic reference/sensing system is based on a series of magnetic markers placed in the center of a predetermined path for a vehicle. Hall effect magnetometers mounted on the front center of the vehicle sense the magnetic field from the markers. Lateral displacement, y , is then determined by an on-board computer based on the magnetic field measurements in the lateral direction, b_h , and the vertical direction, b_v , at the instance the magnetometer crosses the plane of the magnetic marker. See appendix A for a complete list of nomenclature.

The nonlinear characteristics of the components of the magnetic field, b_h and b_v , as functions of lateral displacement are portrayed in [1; Fig. 3] at a **fixed** vertical height, h , of the magnetometer above the magnetic marker.

In a simple case, with fixed h , one method of implementation of the lateral displacement measurement could break the curve of b_v into discrete segments. Thus, a “table look-up” and linear interpolation can approximate the magnitude of lateral displacement, y , from b_v . The sign of y can be determined by the sign of b_h . However, in a realistic situation, the unmeasured height, h , of the magnetometers above the magnetic marker vary substantially while the vehicle is in operation, resulting in very different characteristics of the components of the magnetic field, b_h and b_v , as functions of lateral displacement.

With this issue in mind, a slightly more complicated table look-up approach is suggested. This second method combines both the measurement of b_v and b_h to determine the magnitude of lateral displacement, as well as its direction. As shown in [1] by this method, y becomes a function of b_v and b_h without dependence on the variable height, h . Since the range of h is bounded, it is practical to assume that this method can be implemented by a reasonably sized table look-up and interpolation approach.

Unfortunately, in addition to the magnetic markers, magnetometers also measure magnetic fields from the earth, the vehicle, and possibly other sources, which are combined to define the undesirable magnetic fields, b_u . We can assume that the orientation of the vehicle remains nearly constant between magnetic markers. Thus, the magnetic field from the earth and vehicle remain nearly constant between two markers. Therefore, the measurement of the magnetic field exactly between two magnetic markers should approximately equal b_u . This measured value of b_u can be subtracted from the magnetic field measured directly over a magnetic marker. This results in the isolation of the components b_h and b_v , which in turn determine the lateral displacement.

Experimental results were obtained to evaluate the performance and accuracy of the discrete magnetic marker reference/sensing system. The experimental procedure fixed vertical and horizontal magnetometers at some unknown, but reasonable height above the road surface. A simulated roadway with discrete magnetic markers was guided with known lateral displacements under the magnetometers at nominal longitudinal velocity (see appendix B). Thus, the magnetic field measurement, table look-up and interpolation resulted in a comparison of the true lateral displacement and the measured value as seen in Fig. 1, where the measured points are the average of four lateral displacement measurements from distinct markers. The range of the measurable lateral displacement is ± 8 cm. In this range, the standard deviation of the error was calculated to be 0.4 based on the total number of measurements of each magnetic marker.

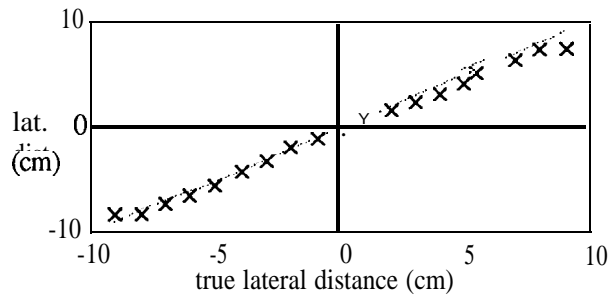


Figure 1: Magnetometer Measurement, $x \Rightarrow$ measured

The major portion of the error is introduced by the linearization of the measured magnetic field vs. lateral displacement characteristics with respect to the *height* of the magnetometers. It is believed that this error can be reduced with careful consideration of the nonlinear behavior of such characteristics in the table look-up scheme.

The block diagram of Fig. 2 shows how the discrete magnetic marker reference/sensing system fits in with the overall lateral control system.

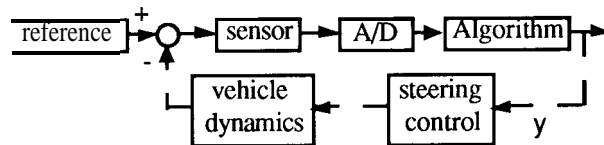


Figure 2: Block Diagram of Control System

3 Dynamic Model

The dynamic modelling of the experimental vehicle was developed in [2]. The details of the experimental vehicle, the sensors, and the computer are presented in [3]. Two models were suggested: a complex nonlinear model and a simplified linear model. Since the bulk of the

nonlinearities arise from tire characteristics of a full-sized car, and since the experimental vehicle simply used a rubber covering over plastic wheels, the nonlinear model was deemed unnecessary. Thus, the linear model was used to simulate vehicle responses as well as to provide a linear plant to design control laws based on linear control theory.

The linear model was obtained by linearizing the nonlinear model. Lateral and yaw motions are the only two motions retained in the linear model. It was confirmed in [2] that simulations of the open loop responses of the detailed nonlinear model and the simplified linear model remained close to each other under typical operating conditions as detailed in Appendix B.

Model verification was confirmed with respect to the experimental vehicle by comparing actual open loop responses to step and sinusoidal front wheel steering angle commands with the simulated prediction of the measurable yaw rate (see Figs. 3 and 4).

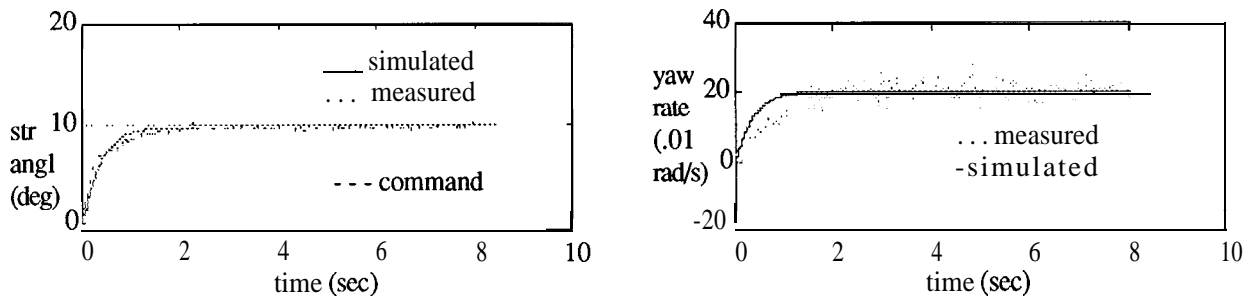


Figure 3: Step Response

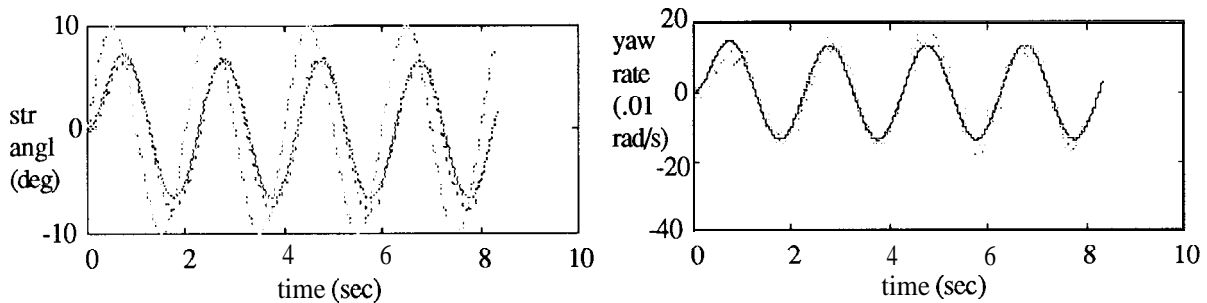


Figure 4: Sinusoidal Response (10 deg ampl, 0.5 Hz.)

Model parameters exist which will vary over a range of values when the vehicle is in operation. These key parameters include the cornering stiffness, C_S , which describe the interaction between the tire and road surface; the load, m and I_z ; and longitudinal velocity, V . Specific numbers for the nominal values and our judgement of an allowable range of values for these key parameters can be found in appendix B, obtained from [3]. The next step is to develop a control law for the lateral motion of the vehicle over the allowable range of key parameters.

4 Lateral Control

The objective of the control law is to achieve good tracking of a predetermined reference path on the roadway, while maintaining smooth ride quality in terms of minimizing lateral acceleration and jerk. Simple PID controllers have been suggested as well as more sophisticated control laws. The main theme of this paper is to show the limitations of the PID control law and thus, the motivation behind a more sophisticated control law.

Fixed PID feedback control gains were obtained from an optimal search method. A performance index consisting of the tracking error and control input was minimized over a series of closed loop simulations with varying PID gains.

A feedforward loop was added to utilize the future information provided by the magnetic markers. As will be detailed later, the future information consists of the location, direction and severity of upcoming curves. The feedforward term adds a steady state front wheel steering angle control term based on vehicle mass, m , longitudinal velocity, V ; estimated cornering stiffness, C_s ; and vehicle geometry, l_1 and l_2 ; (see nomenclature) as well as the radius of curvature, ρ , to the PID feedback control term. The steady state front wheel steering angle, δ_{ss} , can be expressed as a function of the radius of curvature, ρ , by the following [2]:

$$\delta_{ss} = \frac{mV^2(l_2 - l_1) + 2C_s(l_2 + l_1)^2}{2\rho C_d(l_2 + l_1)} \quad (1)$$

Figure 5 shows a block diagram of the PID feedback control system with the feedforward loop, where the input to the plant is the front wheel steering angle command, δ_d , and the output is lateral displacement error, y .

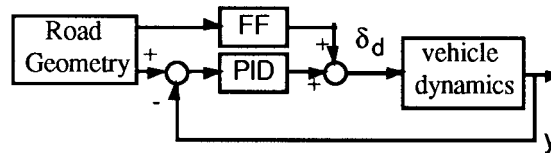


Figure 5: Block Diagram of Control System

Alternative control laws, which have been or are currently under development but have yet to be implemented, are mentioned in the Future Research section.

5 Experimental Car

The experimental vehicle is a highly flexible, computer controlled, 50 kg. scale model car mounted with an array of various sensors [3]. The car is capable of four wheel steering and four wheel drive (4WSD), although only front wheel steering is used for control in the present study. The basic layout of sensors, actuators and the computer on the vehicle can be found in [3; Fig. 1].

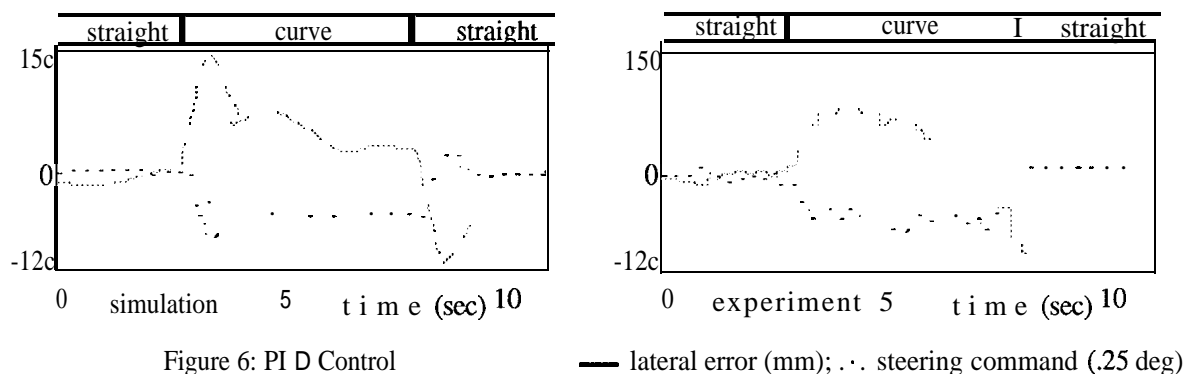
Sensors include rotary encoders and potentiometers on each wheel to measure rotational speeds and steering angles, respectively (see [3] for details). Also included are a yaw rate sensor, lateral accelerometer and longitudinal accelerometer. Finally, two magnetometers are mounted on the front of the vehicle to measure b_v and b_h .

The controller, as well as the reference/sensing system are implemented by an on-board computer based on a Motorola 68020/68881 microprocessing system.

6 Procedure and Results

The objective of the experiment is to test a PID and PID with feedforward control law over an extreme range of operating conditions. The path of magnets on a tiled road surface consisted of a 2.5 meter straight section, a 6.0 meter arc length with a 4.0 meter constant radius of curvature, and a final 2.5 meter straight section. Future roadway information is signaled to the controller by the first magnetic marker. This signal simply turns on a “curve warning” flag. The magnitude and direction of the radius of curvature are encoded in the control software. Test results are presented in this section and discussed in Section 7.

The first test was the simple PID control law under nominal operating conditions (see appendix B). Figure 6 shows the simulated prediction of the lateral displacement and the front wheel steering command (above) as well as the real-time results (below).



The experiment was repeated using a modified control law, adding a feedforward loop and reevaluating the **PID** control parameters to optimize the control objectives (see Fig. 7).

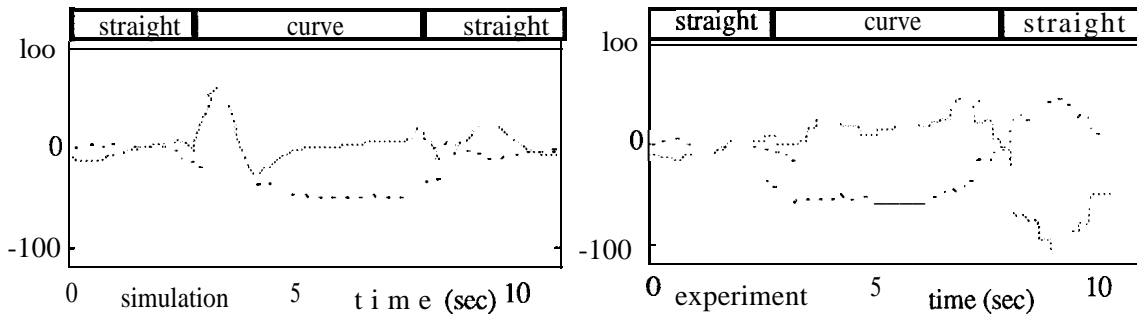


Figure 7: PID/Feedforward Control — lateral error (mm); . . . steering command (.25 deg)

The **PID** and feedforward control law were then tested over difficult operating conditions. Figure 8 shows simulated and experimental results for a load increase on the vehicle of approximately 10 kg. in m and $1 \text{ kg}\cdot\text{m}^2$ in I_z .

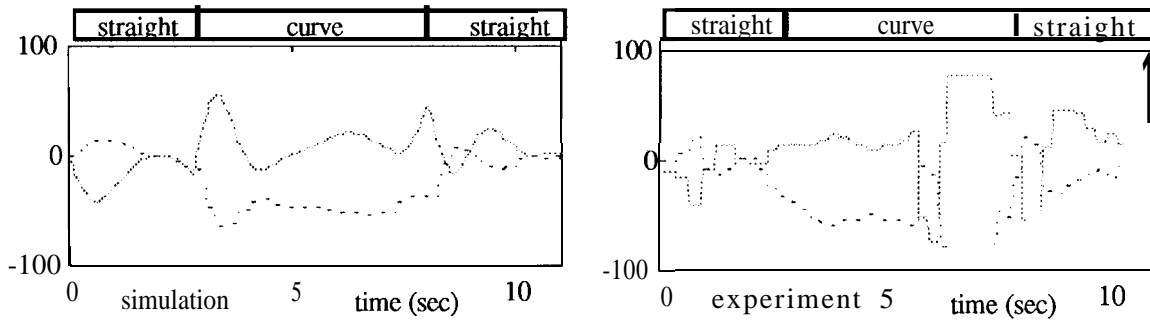


Figure 8: PID/FF Control Δ load — lateral error (mm); . . . steering command (.25 deg)

The results in Fig. 9 are of an increase of longitudinal vehicle speed to 2 m/s, with other vehicle parameters maintaining their nominal values.

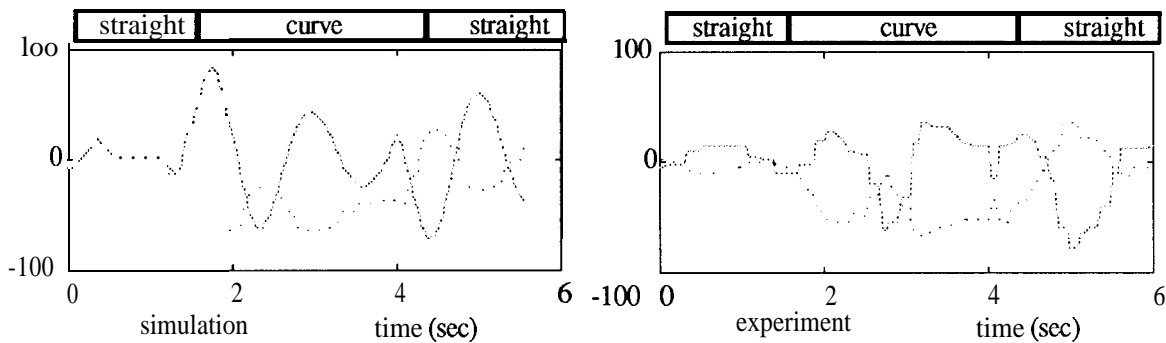
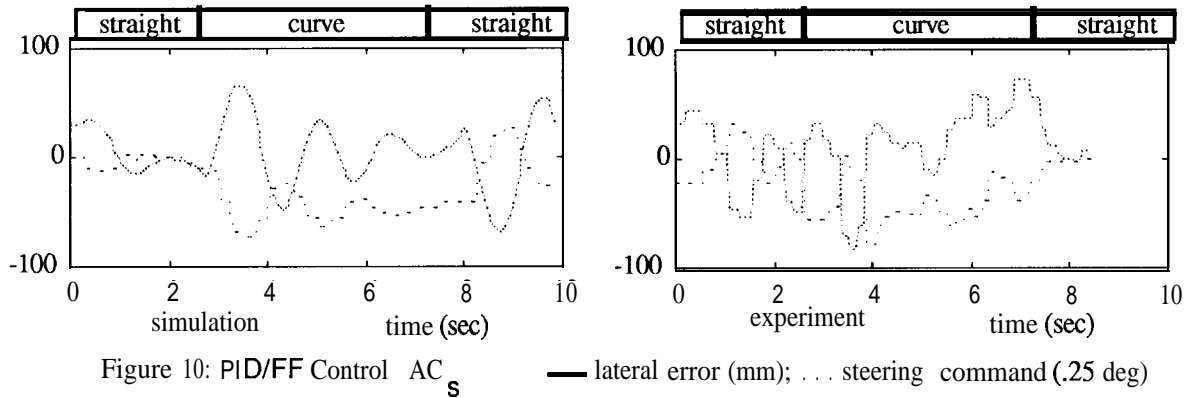


Figure 9: PID/FF Control AV — lateral error (mm); . . . steering command (.25 deg)

Finally, Fig. 10 shows the effect a slippery road surface, and thus a decrease in cornering stiffness to approximately 200 N/radian. This was achieved by adding soapy water to the tiled road surface.



7 Discussion

When a PID controller is used by itself, tracking curved sections is very difficult due to the fact that a correction can only be made after an error has occurred. To maintain tracking on curved sections, simulations indicated a need for large integral action. Although Fig. 6 shows tracking, the large gains cause large overshoot and oscillations in lateral displacement at transitions between straight and curved sections. The experimental result in Fig. 6 shows overshoot exceeding the measurement range.

Clearly there is motivation to take advantage of future information about upcoming roadway geometry provided by the magnetic marker reference/sensing system. The improvement base on the addition of a feedforward loop to the PID controller, was demonstrated in Fig. 7. Large PID gains were no longer required. The lateral displacement response at the transitions between straight and curved sections stabilized much faster than the case without a feedforward control loop. In addition, the average lateral displacement error on the curved section was reduced with the modified controller.

Although this control law performed well under the nominal operating conditions for which it was designed, drastic deviations in the nominal parameters exploited the weaknesses of this control. Simulation predicts that a 20% increase in inertial load to the vehicle will only mildly affect control performance. This conclusion is drawn since the simulation of the closed loop response of the nominal case and the increased load case are similar. However, a typical experimental result shown in Fig. 8 shows large oscillations in lateral error. This difference between the simulation and experimental results of an increase in load of the vehicle may be attributed to some

perturbations of the actual system which are not accounted for in the linear dynamic model, such as a variation in the steering actuator dynamics, a change in cornering stiffness, or a shift in the center of mass of the vehicle.

When the longitudinal velocity, V , was increased to twice the nominal value, the simulation (Fig. 9) predicted very large oscillations in lateral error throughout the entire track. This was confirmed by the experimental results in Fig. 9. Finally, an extreme decrease in cornering stiffness, C_S , (ie. slippery road surface) resulted in highly oscillatory behavior by the **PID/Feedforward** controller in both the simulation and experimental results (see Fig. 10).

8 Future Research

The results of the experiments motivate further research of more sophisticated control laws. One such control law is the Frequency Shaped Linear Quadratic (FSLQ) controller. This controller has the advantage of finding the optimal control law based on a performance index which places frequency dependant weights on the control, tracking error, and lateral acceleration, which is a measure of the ride quality.

Also under development is a fuzzy rule-based controller, which considers the human decision making process in the steering control law, and a sliding controller, which focuses on the improvement of the system robustness characteristics with respect to variations in the key parameters C_S , m , I_z , and V .

9 Conclusion

It has been demonstrated by real time implementation and experimentation that automatic steering control using a discrete magnetic marker reference/sensing system is feasible. Implementation of a **PID** with feedforward control action showed good performance in terms of tracking under nominal conditions. However, the limitations of such a controller were observed as nominal parameters deviated from their nominal values. It is clear that a more sophisticated control law must be developed to handle these parameter changes as well as external disturbances such as wind gusts.

Acknowledgment

The research reported herein is a part of the Program on Advanced Technology for the Highway (PATH), performed under the sponsorship of the State of California Business, Transportation,

and Housing Agency, Department of Transportation, and the U.S. Department of Transportation, Federal Highway Administration.

Appendix A: Nomenclature

- b_h : lateral component of magnetic field of the magnetic marker
- b_v : vertical component of magnetic field of the magnetic marker
- b_u : combined magnetic fields (earth, vehicle), excluding magnetic marker
- γ : lateral displacement
- h : vertical height of the magnetometer above the magnetic the marker
- C_s : cornering stiffness
- m : vehicle mass
- I_z : vehicle moment of inertia about vertical axis
- V : longitudinal velocity
- r : roadway radius of curvature
- δ_d : front wheel steering angle command
- δ_{ss} : front wheel steady state steering angle
- l_1, l_2 : length from vehicle center of gravity to front axle and rear axle, respectively

Appendix B: Nominal Parameters and Range

param.	nom. val.	min.	max.
C_s (N/rad)	1000	200	1000
m (kg)	50	50	60
I_z (kg-m ²)	5	5	6
V (m/s)	1	1	2

References

- [1] Zhang, W., Parsons, R. E., West, T., “An Intelligent Roadway Reference System for Vehicle Lateral Guidance/Control”, 1990 American Control Conference, San Diego, CA., p 281.
- [2] Peng, H., Tomizuka, M., “Vehicle Lateral Control for Highway Automation”, 1990 American Control Conference, San Diego, CA., p 788.

[3] Matsumoto, N. Tomizuka, M., "Vehicle Lateral Velocity and Yaw Control with Two Independent Control Inputs", 1990 American Control Conference, San Diego, CA., p 1868.